Fusion Engineering and Design 160 (2020) 111923

Contents lists available at ScienceDirect

Fusion Engineering and Design

journal homepage: www.elsevier.com/locate/fusengdes

# Backwards extrapolation activation diagnostics and their dynamic range for pulsed neutron source measurements

L.W. Packer[a,*], S. Allan[a], S.C. Bradnam[a], S. Jednorog[b], E. Łaszyńska[b], N.J. Roberts[c], C. Wilson[a], R. Worrall[a]

[a] Culham Centre for Fusion Energy, Culham Science Centre, Abingdon, Oxon OX14 3DB, UK
[b] Institute of Plasma Physics and Laser Microfusion, 01-497 Warsaw, Poland
[c] National Physical Laboratory, Teddington TW11 0LW, UK

ARTICLE INFO

*Keywords:*
Activation
Neutron
Pulsed fields

ABSTRACT

Activation materials implanted within radiation detectors can be used to measure pulsed neutron fields. This work develops an instrument concept with the aim to maximise sensitivity to pulsed fusion neutron fields and, using a data-rejection algorithm combined with backwards extrapolation, enable neutron fluence estimates to be made over a large dynamic range. Through high-fidelity modelling of residual temporal emissions, and a parameterised approach, we study the sensitivity to neutrons of a plastic scintillator–Ag foil layer detector concept. For an optimal design we apply paralysable and non-paralysable deadtime models to the predicted response to D–D fusion neutron fields at various neutron field intensities. In high neutron fluence irradiation scenarios, where deadtime effects are strongly evident, we use our approach to make estimates of the fluence from instrument response data. We discuss the practical applications of such diagnostics used for plasma focus (PF) fusion experiments, such as at the PF-1000U facility in IPPLM, Poland, inertial confinement fusion and pulsed tokamak experiments, for example at MAST-U, where such diagnostics could complement fission counter-based neutron diagnostics in the future. Finally, we show that the calibration of such detection systems may be achieved using relatively low emission rate, steady state neutron sources, with calibration factors that are straightforward to apply to pulsed neutron field measurements.

## 1. Introduction

The measurement of fusion neutron yields provides a direct relationship with fusion power and is hence an important measure of experimental performance. In pulsed neutron emission scenarios, such as those experienced in dense plasma focus devices or inertial confinement fusion experiments—where pulse durations are on the nanosecond timescale—several considerations in selecting a suitable diagnostic must be made. These include the sensitivity to neutrons, immunity to electromagnetic interference, linearity of neutron fluence measurement across a dynamic range, but also practicalities such as how to ensure a reliable calibration across this range. Integrated fluence detection systems such as activation foils, CR39 and bubble detectors for example are often the primary choice for such measurements. However, due to intermediate, often manual steps as part of the measurement process, some of these systems have drawbacks over integrated pulse counting or current-based detection systems which allow for real time data acquisition. Activation foils, such as silver, combined with active detection systems such as Geiger-Müller (G-M) tubes or proportional counters [1], utilise the $^{107}$Ag(n,$\gamma$)$^{108}$Ag and $^{109}$Ag(n,$\gamma$)$^{110}$Ag reactions that have been widely and successfully used, and provide the convenience of an integrated diagnostic with post-pulse data output. Efficiency increases may be obtained via moderating neutrons via a hydrogenous moderator such as high density polyethylene, thereby increasing the Ag neutron capture probability. This type, and other activation-based diagnostics, particularly threshold reactions e.g. $^{115}$In(n,n')$^{115m}$In and $^{89}$Y(n,n')$^{89m}$Y, have been explored extensively in research groups to measure quantities such as the total neutron yield and neutron angular distribution from Plasma Focus discharge devices, such as the PF-1000U (see Fig. 1) and PF-6 devices in Poland [2–5]. The PF-1000U device operates with the vacuum vessel filled with deuterium with discharge current up to 2 MA. The plasma pinches typically last 100–200 ns with plasma temperatures in the region of 1 keV, density of the order $10^{19}$ cm$^{-3}$ with resultant emissions of up to $10^{12}$ n/pulse [3] with energy around 2.5 MeV.

In this work we explore, via a parameterised radiation transport

* Corresponding author.
*E-mail address:* lee.packer@ukaea.uk (L.W. Packer).

https://doi.org/10.1016/j.fusengdes.2020.111923
Received 17 September 2019; Accepted 25 July 2020
0920-3796/ © 2020 The Authors. Published by Elsevier B.V. This is an open access article under the CC BY-NC-ND license (http://creativecommons.org/licenses/BY-NC-ND/4.0/).

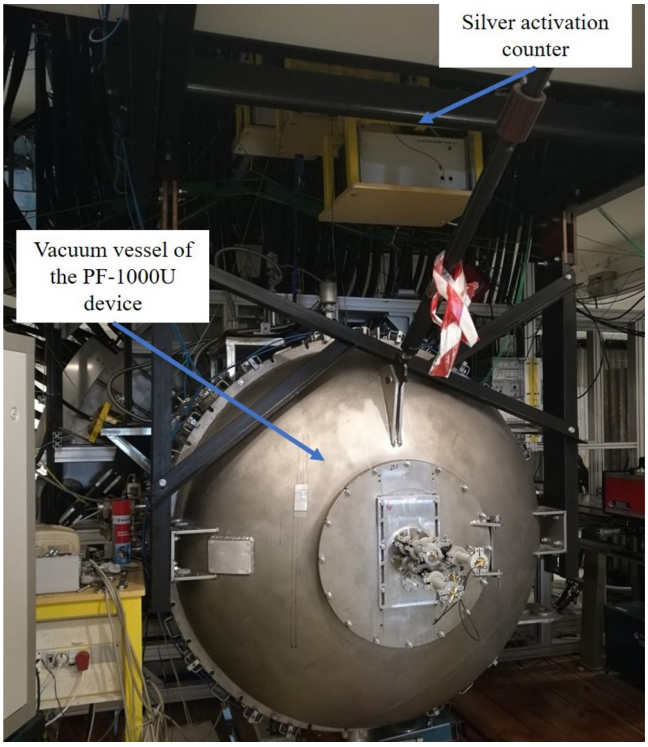


**Fig. 1.** Image of the PF-1000U device vacuum vessel also showing the G–M tube-based silver activation diagnostic position, described in detail in [3].

model, the predicted response to incident neutrons and subsequent $\beta^-$ emissions of an activation foil–scintillator sandwich detector concept. Using a detector configuration optimised for response as a basis we then predict the temporal count rate behaviour to incident neutron pulses of varying yield incorporating standard dead-time models. We apply a basic data-rejection algorithm with the aim to exclude high deadtime-impacted (count rate) data points at short times following the neutron pulse. At longer times, using a backwards extrapolation approach acting on the 'reliable' count rate data, we derive the incident neutron yield.

## 2. Activation foil–scintillator sandwich model

We have developed an integrated modelling approach to simulate the response to incident neutrons of a sandwich arrangement of Ag activation foils embedded into plastic scintillator media (such as EJ-200). The simulation approach uses the MCNP6.2 [6] radiation transport code for neutron and electron transport in a two-step calculation. Fig. 2 shows a schematic of the detector configuration concept with activation foil–scintillator layer dimensions. In the first calculation step we have estimated the relevant activation reaction response in each activation foil layer to a plane parallel beam configuration of incident neutrons with 2.45 MeV energy. In a second calculation step we have implemented the decay radiation energy field and intensity per foil layer into the model (i.e. the $\beta^-$ emission spectra) and have used pulse height tallies (the F8 tally in MCNP6) applied to the scintillator regions, also applying an energy threshold (ranging from 0.1–0.5 MeV) to evaluate the overall response. The nuclear data used in the MCNP6 calculations were FENDL-3.1b [7]. The $\beta^-$ emission spectra for $^{108}$Ag and $^{110}$Ag are from [8], which were implemented into electron source definitions within the MCNP6 code for the second stage of the calculation to determine the events induced by $\beta^-$ emissions originating in the Ag foil within the scintillator.

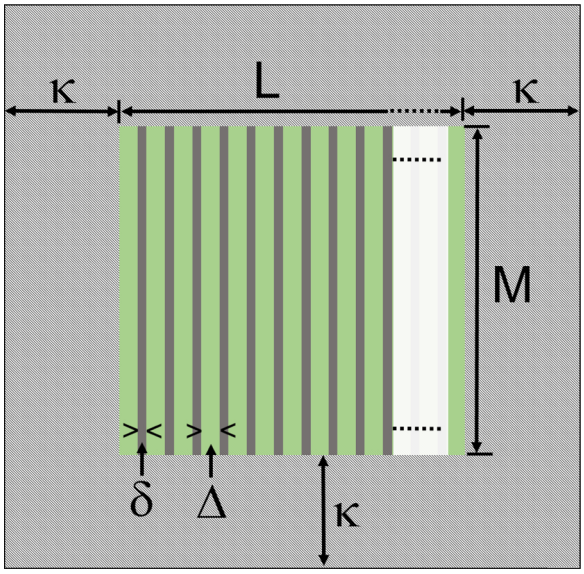


**Fig. 2.** Schematic of the parametric detector model developed and used in this work. $\kappa$ is the polyethylene front moderator depth parametric variable; $M$ is the layered detector cell height and depth (10 cm in our case); $L$ is the layered detector cell depth (an integer number of layers less than or equal to 10 cm); $\delta$ is the foil thickness parametric variable and $\Delta$ is the scintillator thickness parametric variable.

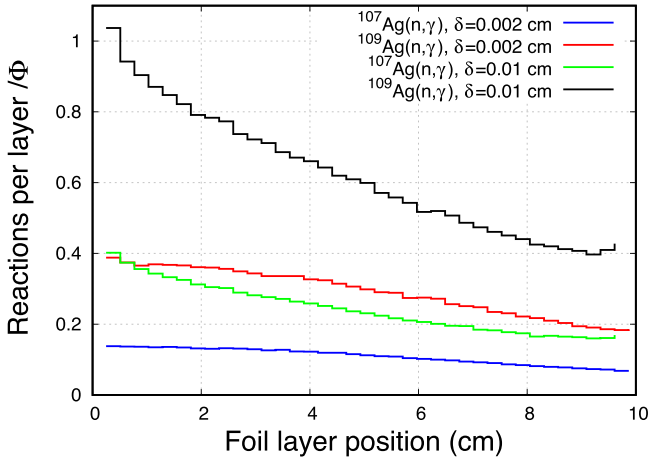


**Fig. 3.** Reaction per foil layer per fluence for $\delta = 0.01$ and 0.002 cm; $\Delta = 0.25$ cm; threshold = 0.5 MeV.

### 2.1. Results from parameterised model simulations

Using a scripted approach to simulations we have explored responses to model variations in $\delta$ in the range 20–100 μm, $\Delta$ in the range 0.05–0.25 cm and $\kappa$ in the range 1–4 cm. Fig. 3 shows the reactions per foil layer through the model per incident fluence for two different foil thicknesses. The black and green curves show that the 100 μm foil case provides a higher overall response at all layer positions compared to the 20 μm case.

Fig. 4 shows the moderator thickness versus intrinsic efficiency, $\varepsilon$, for the range of $\delta$ and $\Delta$ values evaluated. In all cases the $\kappa = 3$ cm moderator thickness yielded the highest intrinsic efficiency. Fig. 5 shows the total Ag mass versus intrinsic efficiency using $\kappa = 3$ cm for all $\delta$ and $\Delta$ values that were explored. The optimum Ag mass to give the highest intrinsic efficiency is around 390–400 g. In other words combinations of scintillator thickness, $\Delta$, and foil thickness, $\delta$, which equate to this total Ag mass tend to yield the maximum intrinsic efficiency. In

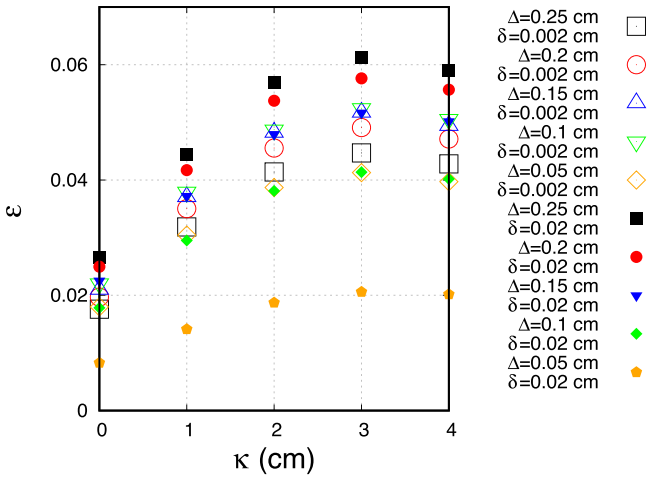


**Fig. 4.** Moderator thickness versus intrinsic efficiency, $\varepsilon$, for the full range of $\delta$ and $\Delta$ values with threshold = 0.5 MeV.

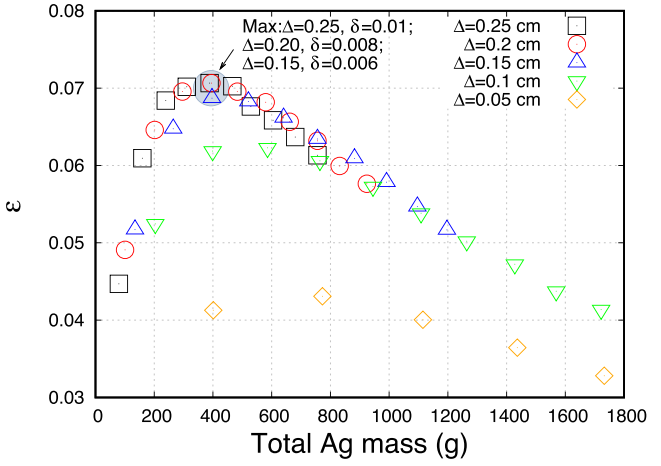


**Fig. 5.** Total Ag mass versus intrinsic efficiency, $\varepsilon$, for the full range of $\Delta$ values with threshold = 0.5 MeV.

our case the depth of the detector is constrained to an integer number of layers less than or equal to 10 cm —hence the scintillator thickness effectively determines the number of Ag foil layers. The case: $\delta$ = 0.01 cm; $\Delta$ = 0.25 cm marginally gave the highest value and was selected for further detailed study in later sections.

### 2.2. Calibration methodology

Calibration of an activation-based neutron instrument is straightforward to perform using a relatively low emission rate (steady state) calibration field. This is fortunate since pulsed calibration neutron standards have not been widely developed. An ideal field for calibration of our concept instrument in our particular application is a monoenergetic neutron field of 2.45 MeV. At the National Physical Laboratory (NPL), such a field of neutrons may be produced by accelerating a beam of 3.27 MeV protons using a Van de Graaff generator onto a neutron producing target utilising the T(p,n)$^3$He reaction to produce 2.45 MeV neutrons at 0° to the beam direction. Calibration factors derived from steady state measurements may then be applied with some confidence to pulsed operations. To illustrate the behaviour, the predicted characteristic response of our detector when exposed to a 2.45 MeV plane parallel source with an incident known flux of $\phi_{exp}$ = 1000 n cm$^{-2}$ s$^{-1}$ is shown in Fig. 7. Two components of the response can be seen due to $^{107}$Ag(n,$\gamma$)$^{108}$Ag and $^{109}$Ag(n,$\gamma$)$^{110}$Ag

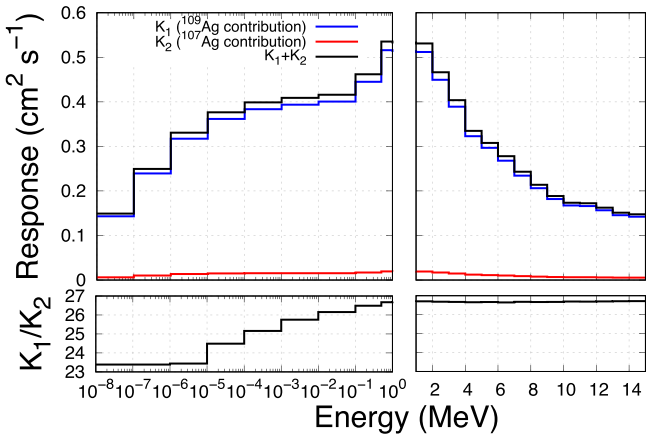


**Fig. 6.** Total, $K_1$ and $K_2$ response rate with energy for the $\delta$ = 0.01 cm; $\Delta$ = 0.25 cm; $\kappa$ = 3 case.

reactions. By fitting the two saturation parameters, $A_1$ and $A_2$, using

$$M_{t_n} = A_1(1 - e^{-\lambda_1 t_n}) + A_2(1 - e^{-\lambda_2 t_n}) \quad (1)$$

to $M_{t_n}$, the average measured count rate per $n$th time bin at time $t_n$, during neutron irradiation (here using a constant emission neutron source) can be derived. One can determine the corresponding calibration response factors by dividing the derived $A_1$ and $A_2$ values by $\phi_{exp}$ i.e. $K_1 = A_1/\phi_{exp}$ and $K_2 = A_2/\phi_{exp}$. In this case the instantaneous response rate (immediately following the incident pulse) per neutron fluence is 0.434 cm$^2$ s$^{-1}$, with 96.6% of this from the $^{109}$Ag(n,$\gamma$)$^{110}$Ag reaction. The $^{108}$Ag and $^{110}$Ag components of this response rate may then be integrated over all cooling times to yield a maximum overall response of 18.1 cm$^2$, suggesting that neutron fluences of 500 n cm$^{-2}$ will be measurable with a Poisson statistical uncertainty of about 1%. Since the experimental calibration would be performed using a divergent neutron beam, the effective centre of the instrument would need to be determined in order to properly determine the experimental incident neutron fluence used in the calibration itself. This may be performed from a series of experimental measurements at a range of distances, or via MCNP calculations.

Other commonly available neutron sources, such as $^{252}$Cf, $^{241}$Am–Be may be used for calibration of this instrument, although a small response correction for neutron spectrum is necessary. Fig. 6 shows the calculated instantaneous response rate (immediately following the incident pulse) per neutron fluence for the $\delta$ = 0.01 cm; $\Delta$ = 0.25 cm;

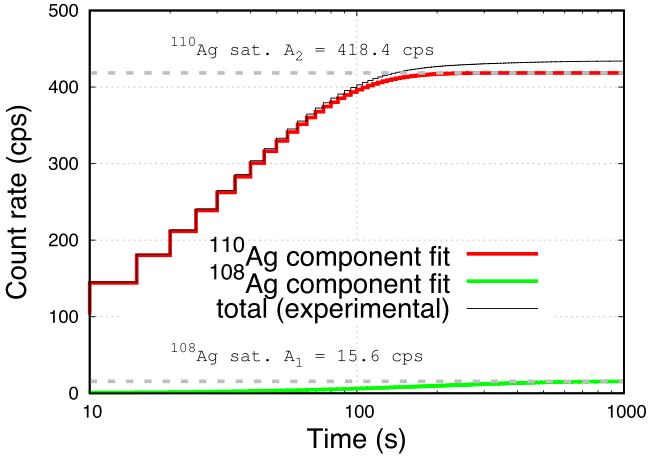


**Fig. 7.** Simulated instrument response during irradiation with steady state source with incident fluence of 1000 n cm$^{-2}$ s$^{-2}$. Response factors for the $^{107}$Ag(n,$\gamma$)$^{108}$Ag and $^{109}$Ag(n,$\gamma$)$^{110}$Ag components may be derived from fitting to the experimental data.

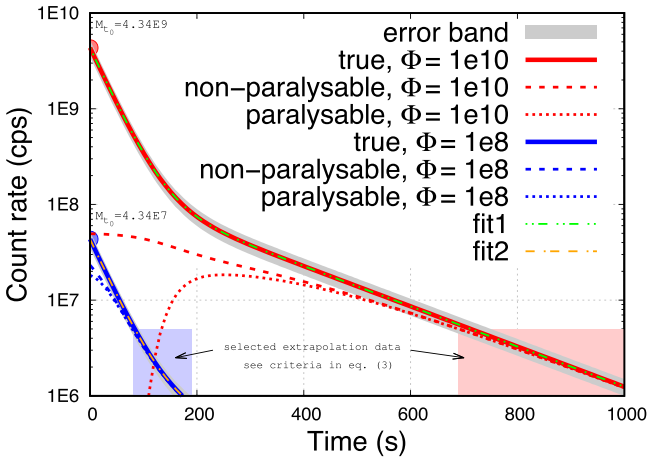


**Fig. 8.** Simulated instrument response versus time for paralysable and non-paralysable deadtime models following various incident neutron pulse yields. Results are compared to the true response. Curves have been fitted, with uncertainty bands, to each set to selected data points within the rectangular regions, to determine $M_{t_0}$ (and hence $\phi_0$).

$\kappa = 3$ case. The function can be folded with both the calibration and measurement spectra to calculate the necessary correction factor. One can observe in Fig. 6 that the response is highest around approximately 1 MeV and is dominated by the $^{109}$Ag(n,$\gamma$)$^{110}$Ag contribution. Whilst the $^{107}$Ag(n,$\gamma$)$^{108}$Ag contribution is smaller, in pulsed measurements this contribution would eventually dominate the overall total response at times exceeding approximately 140 s following the incident neutron pulse, due to the different decay constants of $^{108}$Ag and $^{110}$Ag. The ratio $K_1/K_2$ is relatively constant, approximately 26.7, above 1 MeV. This is convenient since it shows that the calibration neutron spectrum does not particularly affect the ratio.

## 3. Deadtime and count rate response modelling

Detectors that operate in pulse counting mode experience deadtime effects. Events that occur within the deadtime are lost, i.e. not counted, resulting in reduced count rates. In general the characteristic deadtime behaviour for a particular detector system must be corrected for. We apply paralysable and non-paralysable deadtime models that are well described by [9,10] to our developed detector concept. For our detection system we have assumed a deadtime, $\tau$, of 20 ns which is in the typical range for a fast scintillator. We have used the optimised model case where $\delta = 0.01$ cm, $\Delta = 0.25$ cm and threshold = 0.5 MeV to perform the following analyses. Fig. 8 shows the simulated instrument temporal response, using the two deadtime models following various incident neutron pulse fluences of $10^8$ and $10^{10}$ n cm$^{-2}$. These predictions are compared with the true theoretical response (i.e. assuming no deadtime losses) and one can see particularly large deviations from the true response in the case where $\phi_0 = 10^{10}$ n cm$^{-2}$.

One can determine $\phi_0$ experimentally from a weighted fit over selected measurements at different $t_n$. For pulsed neutron measurements one can use the calibration factors, $K_1$ and $K_2$, derived from fitting Eq. (1) to make $n$ estimates of the total neutron fluence, $\phi_0$, via measurements, $M_{t_n}$, at times $t_n$.

$$\phi_0 = \frac{M_{t_n}}{\left(K_1 e^{-\lambda_1 t_n} + K_2 e^{-\lambda_2 t_n}\right)} \tag{2}$$

It is advisable to avoid using measurement data where deadtime losses are particularly high (i.e. deviations >10% from the true rate), especially since $\tau$ may be uncertain or subject to variation, and the system may not follow deadtime-loss models exactly. To minimise the effects of these uncertainties we have implemented a simple data acceptance algorithm to test each $M_{t_n}$ value via two conditional tests:

$$\frac{M_{t_{n+1}} - M_{t_n}}{t_{n+1} - t_n} < 0;\ M_{t_n} < \frac{1}{10\tau} \tag{3}$$

The first condition is a gradient test, to ensure the gradient is negative, the second test is a count rate limit based on the expected deadtime of the system. Fig. 8 shows two highlighted (blue and red) rectangular regions for each of the two incident fluence levels. These regions show data where the above conditions are true and, hence, the data has been used for extrapolation. The respective data sets have been deadtime corrected and used with Eq. (2) to determine $\phi_0$ in each case.

## 4. Discussion and conclusions

We have developed a scintillator–Ag foil detector concept with the aim to maximise sensitivity to pulsed fusion neutron fields. Via a parameter study we have selected a detector configuration with foil, scintillator and moderator thicknesses of 0.01, 0.25 and 3 cm respectively with an energy threshold of 0.5 MeV. This gave the highest overall instantaneous response rate to incident 2.45 MeV neutrons of 0.434 cm$^2$ s$^{-1}$. The $^{108}$Ag and $^{110}$Ag components of this response rate may be integrated over all cooling time to yield a maximum response of 18.1 cm$^2$, suggesting that neutron fluences of 500 n cm$^{-2}$ will be measurable with an uncertainty of approximately 1%. Conversely, at higher fluences where deadtime effects are strongly manifest, we predict how the instrument responds temporally. Via a data-rejection algorithm to select 'reliable' instrument response data and backwards extrapolation we demonstrate conceptually how neutron fluence estimates may be made. We have explored a case with $10^{10}$ n cm$^{-2}$ s, though higher fluences should in principle be possible to measure. A drawback is that for large neutron fluences timescales on the order of a few minutes—the time increasing with neutron fluence—are needed to wait for acceptable data, then fully collect and process it. However, within facilities where the number of experimental shots does not exceed a few 10 s pulses per day this is not a significant disadvantage.

The primary application of this instrument is to measure short pulse fusion neutron fields such as those associated with plasma focus device or inertial confinement fusion experiments. However, in pulsed tokamak operations the scintillator–Ag detector concept also has potential to complement existing fission counter based neutron yield detection systems, which is currently the primary means of determining neutron yield at MAST-U. Since fission counter diagnostics are required to measure fusion neutron yield across a large neutron yield range they are configured to switch from pulse counting mode, in low neutron fluence fields, to current mode in larger fields. Whilst fission counters can be readily calibrated in pulse counting mode using low intensity neutron field standards, the calibration in current mode is more challenging due to the present lack of availability of high intensity neutron fields. A benefit of the activation concept we describe is that only pulse counting mode is used to determine the neutron fluence resulting from the pulse. In this work we have shown that calibration in low intensity, steady state neutron fields is achievable and the derived calibration factors are straightforward to apply to pulsed neutron field measurements.

## Declaration of Competing Interest

The authors declare that they have no known competing financial interests or personal relationships that could have appeared to influence the work reported in this paper.

## Acknowledgements

Work supported by RCUK [grant number EP/P012450/1] and the Euratom Research and Training Programme.

## References


[1] P. Dighe, D. Das, Annular shape silver lined proportional counter for on-line pulsed neutron yield measurement, Nucl. Instrum. Methods Phys. Res. Sect. A 778 (2015) 115–119.

[2] S. Jednorog, et al., Preliminary determination of angular distribution of neutrons emitted from PF-1000 facility by indium activation, Nukleonika 57 (2012) 563–568.

[3] S. Jednorog, et al., The application of selected radionuclides for monitoring of the D-D reactions produced by dense plasma-focus device, J. Radioanal. Nucl. Chem. 301 (2014) 23–31.

[4] B. Bienkowska, et al., Measurements of neutron yield from PF-1000 device by activation method, Czechoslov. J. Phys. 5756 (2006) B377–B382.

[5] V.A. Gribkov, et al., Examination of a chamber of a large fusion facility by means of neutron activation technique with nanosecond neutron pulse generated by dense plasma focus device PF-6, Fusion Eng. Des. 125 (2017) 109–117.

[6] D.B. Pelowitz, et al., MCNP6 User's Manual Version 1, Los Alamos Document Number: LA-CP-13-00634, Rev. 0, (2013).

[7] IAEA, Fusion Evaluated Nuclear Data Library ver. 3.1. https://www-nds.iaea.org/fendl/.

[8] Nuclear Data Sheets for A = 110, Nuclear Data Sheets 113 (5) (2012), 1315–1561.

[9] A. Talamo, Y. Gohar, Application of the backward extrapolation method to pulsed neutron sources, Nucl. Instrum. Methods Phys. Res. Sect. A 877 (2018) 16–23.

[10] E. Gilad, et al., Dead time corrections using the backward extrapolation method, Nucl. Instrum. Methods Phys. Res. Sect. A 854 (2017) 53–60.